Published in final edited form as:

Mol Genet Metab. 2016 September ; 119(1-2): 144–150. doi:10.1016/j.ymgme.2016.07.010.

Development of a model system for neuronal dysfunction in Fabry Disease

Christine R. Kaneski, MS[a,*], **Roscoe O. Brady, MD**[a], **John A. Hanover, PhD**[b], and **Ulrike H. Schueler, PhD**[b]

[a]National Institute of Neurological Disorders and Stroke, National Institutes of Health, Bethesda, MD, 20892, USA

[b]National Institute of Diabetes and Digestive and Kidney Diseases, National Institutes of Health, Bethesda, MD, 20892, USA

Abstract

Fabry disease is a glycosphingolipid storage disorder that is caused by a genetic deficiency of the enzyme alpha-galactosidase A (AGA, EC 3.2.1.22). It is a multisystem disease that affects the vascular, cardiac, renal, and nervous systems. One of the hallmarks of this disorder is neuropathic pain and sympathetic and parasympathetic nervous dysfunction. The exact mechanism by which changes in AGA activity result in change in neuronal function is not clear, partly due to of a lack of relevant model systems. In this study, we report the development of an *in vitro* model system to study neuronal dysfunction in Fabry disease by using short-hairpin RNA to create a stable knock-down of AGA in the human cholinergic neuronal cell line, LA-N-2. We show that gene-silenced cells show specifically reduced AGA activity and store globotriaosylceramide. In gene-silenced cells, release of the neurotransmitter acetylcholine is significantly reduced, demonstrating that this model may be used to study specific neuronal functions such as neurotransmitter release in Fabry disease.

Keywords

Acetylcholine; Alpha-galactosidase A; Fabry Disease; Gene Silencing; Neuropathy

1. Introduction

Fabry disease is an X-linked glycosphingolipid-storage disorder caused by a deficiency of the lysosomal enzyme α-galactosidase A (AGA, EC 3.2.1.22). As a consequence of reduced activity of this enzyme, globotriaosylceramide (Gb3), and to a lesser extent, galabiosylceramide, accumulate in the cells of most tissues and organs resulting in a multi-system pathology which frequently includes neurological symptoms [1]. To date, over 600

*Corresponding author: National Institutes of Health, Bldg. 8, Room 422, Bethesda, MD 20892, phone: 301-594-5084, kaneskic@ninds.nih.gov.

mutations in the *GLA* gene for AGA expression have been described which result in variable expression of the symptoms of Fabry disease depending on the amount of residual activity in the mutant AGA protein [2].

In its classic form, Fabry disease includes signs and symptoms such as angiokeratoma, corneal clouding, reduced sweating, hearing loss, abdominal pain, diarrhea, neuropathic pain, cardiac hypertrophy, progressive kidney failure, and stroke, and causes significant morbidity even in childhood.

The neurological manifestations of Fabry disease include both peripheral nervous system and CNS involvement [3]. One of the most debilitating symptoms of Fabry disease is severe neuropathic pain that is poorly controlled by currently available pain medications. In addition, the patients experience symptoms of autonomic dysfunction such as reduced sweating, gastrointestinal pain, and changes in gastrointestinal motility and cardiac rhythm [4]. In autopsy findings, autonomic centers throughout the nervous system show increased Gb3 storage by immunohistochemical staining [5]. In skin biopsy studies, Fabry patients show severe loss of intra-epidermal innervation associated with a small-fiber sensory neuropathy [6]. Although enzyme replacement therapy (ERT) with AGA is currently available to treat Fabry disease, even long-term treatment does not completely reverse the neurologic dysfunction found in these patients [7].

The mechanism by which deficiency in AGA activity results in changes in neuronal function is not clear. Neuronal storage of Gb3 is found in dorsal root ganglia neurons in Fabry disease, and it is suggested that this contributes to the peripheral neuropathy [8]. A Gb3 metabolite, globotriaosylsphingosine (lyso-Gb3), which is the deacylated form of Gb3, is dramatically increased in plasma of classically affected male Fabry patients and in plasma and tissues of Fabry mice [9]. These high levels of lyso-Gb3 may also contribute to the pathology of Fabry disease and may be a reason for the painful damage to dorsal root ganglia neurons. Recently, Choi et al. demonstrated that direct application of lyso-Gb3 sensitized nociceptive neurons in the foot pads of normal mice and that lyso-Gb3 increased Ca^{2+} influx in normal dorsal root ganglion cells cultured from adult mice [10]. In a related lysosomal storage disorder, Gaucher disease, we have shown that glucosylsphingosine (glucopsychosine), an analog of lyso-Gb3, is toxic to cultured neuronal cells [11].

While previous work has documented the accumulation of Gb3 and associated lipids in nervous tissue in autopsy specimens of Fabry patients [5,8] and numerous studies have characterized the small fiber neuropathy and nervous system dysfunctions found in Fabry patients (see [12] for a review), attempts to study these changes on a molecular level have been lacking, in part because a suitable model system is unavailable. Lakoma *et al.* recently published a study with the Fabry mouse model showing that GLA knock-out mice have many features of peripheral neuropathy found in Fabry patients [13], but there have been no studies with human neuronal systems. With the development of gene silencing techniques, it is now possible to create genetically-engineered cell lines to study the mechanisms of neuronal dysfunction in Fabry disease. To create such an *in vitro* model system, we used gene silencing with short-hairpin RNA to generate a stable knock-down of AGA in LA-N-2,

a human neuroblastoma that can be differentiated to neuronal-like cells with characteristics of cholinergic neurons [14].

2. Materials and Methods

2.1 Cell Culture

LA-N-2 cells were a gift from Dr. JK Blusztajn, Boston University, Boston, MA. They were maintained on DMEM/F12 medium supplemented with 15% GemCell Super Calf Serum (GCS, Gemini Bioproducts, Sacramento, CA), 1% non-essential amino acids and 1% penicillin/streptomycin. Growth medium was replaced every 2–3 days, and the cells were subcultured when approximately 80% confluent.

2.2 Gene Silencing

Mission™ plasmid shRNA TRCN0000303790 [15] containing a short-hairpin RNA sequence targeting alpha-galactosidase (NM_000169.2) at nucleotide 458, was obtained as a glycerol stock from Sigma-Aldrich Chemical Company, St. Louis, MO. The plasmid contains a sequence-verified shRNA in the TRC2-pLKO-puro vector.

LA-N-2 cells in log-phase growth were seeded in 6-well plates in growth medium. After overnight incubation, cultures were transfected with 2.5 μg purified plasmid complexed with 1.5 μl Omni Ultra-Transfect™ Transfection Reagent (DBio, LLC, Baltimore, MD) according to the manufacturer's directions. After 48 hrs, the cells were trypsinized and reseeded in a 100 mm dish in growth medium without antibiotics supplemented with 0.6 μg/ml puromycin (selection medium) for 6 days, followed by selection in 1.0 μg/ml puromycin for an additional 7 days. The cells were refed with selection medium every other day. The surviving colonies were expanded in growth medium without puromycin and tested for AGA activity. The colony with the lowest activity (Clone 7) was subcloned by serial dilution and colonies were expanded in selection medium with 3.0 μg/ml puromycin for 13 days.

To control for non-specific effects, LA-N-2 cells were also transfected with a control shRNA plasmid that encodes a scrambled shRNA sequence that will not lead to the specific degradation of any known cellular mRNA. (Control shRNA Plasmid-A, Santa Cruz Biotechnology, Dallas, TX) using the same procedure.

2.3 Neuronal Differentiation

For some experiments, LA-N-2 cells were differentiated using a modification of the method of Zineman et al. [16]. Cells were plated in either 2-well glass slides for immunostaining or plastic tissue culture plates at a density of 32,000 cells/cm^2 in growth medium. After overnight incubation to allow the cells to adhere, the cultures were gently washed twice with PBS and refed with Neurobasal™ medium (Gibco) supplemented with glucose (2 mg/ml), GlutaMAX™ (0.5 mM, Gibco), GCS (1%), B27 supplement (2%, Gibco), retinoic acid (3 ug/ml), forskolin (25 uM), recombinant human nerve growth factor (10 ng/ml), CNTF (10 ng/ml), and choline (100 uM). Cultures were incubated for a minimum of 4 days or until the cells stopped proliferating and formed elongated processes. Medium was changed every 2–3 days as necessary.

2.4 Measurement of AGA activity in cell extracts

A standard uorometric assay for AGA in cell extracts was performed as previously described [17] with modifications. Brie y, cell pellets were resuspended in citrate-phosphate buffer (pH 4.6) containing sodium taurocholate (5 mg/ml) and Triton-X 100 (0.1%). The suspensions were frozen (−20°C) and thawed once, then centrifuged at 5,000 × g for 5 min. Aliquots of the supernatant were incubated for one hour with 4-methylumbelliferyl-alpha-D-galactopyranoside (5 mM, Research Products International, Mount Prospect, IL) in citrate-phosphate buffer (pH 4.6) in the presence of N-acetyl-galactosamine (0.1 M, Research Products International), a specic inhibitor of alpha-galactosidase B [18]. At the end of the incubation period, enzyme activity was stopped with glycine buffer (0.1 N, pH 10.6). Fluorescence in samples was determined using a CytoFluor 4000 plate reader (Applied Biosystems, Foster City, CA) with an excitation lter of 360 nm and emission lter of 490 nm. Amount of product formed was determined using 4-MU standards diluted in 0.1 N glycine stop buffer. Protein levels in extracts were determined using the BCA protein assay kit (Pierce, Rockford, IL) according to the manufacturer's instructions. AGA activity was calculated as nmoles 4-MU formed/hour/mg protein and results were compared to untransfected controls included in the same assay.

2.5 Immunostaining and Flow Cytometry

For immunostaining, LA-N-2 cells were seeded on 2-well glass slides and differentiated. At the end of the incubation they were fixed with 3% paraformaldehyde and stained by indirect immunofluorescence as previously described [19] using saponin as a permeabilizing agent. For Gb3, cells were stained with a mouse monoclonal antibody to Gb3 (BGR 23, Seikagaku Corp, Falmouth, MA) at a dilution of 1:500 and was detected with Alexa Fluor 488 goat anti-mouse IgG (Molecular Probes). For the pan-neuronal marker, PGP 9.5, cells were stained with guinea pig polyclonal anti-PGP 9.5 antibody (GeneTex, Inc., Irvine, CA) at a dilution of 1:500 which was detected with Alexa Fluor 594 goat anti-guinea pig IgG (Thermo Scientific, Rockford, IL). Slides were imaged with a Keyence BZ-9000 fluorescence microscope with a 20× objective. To control for non-specific staining, all immunostaining experiments included a negative control culture that was stained in parallel with only the appropriate secondary antibody (with Alexa Fluor 488 goat anti-mouse IgG or Alexa Fluor 594 goat anti-guinea pig IgG), but no primary antibody.

For flow cytometry for Gb3 staining, undifferentiated cultures were trypsinized, and cell suspensions were fixed with 2% paraformaldehyde and stained as described for slides except the Gb3 antibody was detected with PE-labeled goat F(ab′)2 anti-Mouse IgG (EMD Millipore, Bellerica, MA). As a control for non-specific staining, an aliquot of each cell line was stained in parallel with only PE-labeled goat F(ab′)2 anti-Mouse IgG but no primary antibody. Stained cells were analyzed using a Guava PCA flow cytometer (EMD Millipore). Results were extracted into FACS 2.0 files and graphed using GraphPad Prism 4.0 for Windows (GraphPad Software, La Jolla CA).

2.6 Quantitative RT-PCR

Isolation of total RNA from cultured cells was performed using a PureLink® RNA extraction kit (Ambion). DNA contamination was removed by treating an aliquot of the

extracted RNA with RTS DNase kit (MoBio, Carlsbad, CA) according to the manufacturer's instructions. Amount of RNA was quantified using a Nanodrop 1000 spectrophotometer (Nanodrop Products, Wilmington, DE) and 10 ug of RNA was converted to cDNA using ABI High Capacity cDNA Reverse Transcription Kit (Applied Biosystems, Foster City, CA) with random hexamers. PCR was performed in duplicate samples with cDNA equivalent to 100 ng of original RNA using LuminoCt® SYBR® Green qPCR ReadyMix (Sigma-Aldrich, St. Louis, MO) and QuantiTect® primers (Qiagen, Valencia, CA) for either human GLA or B2M. Reactions were run in a CFX96 Touch™ Real-Time PCR Detection System (BioRad, Hercules, CA) under the following parameters: 95.0 C for 20 s; 40 cycles at 95.0 C for 5 s; 61.0 C for 30 s; followed by a melt curve from 60.0 to 95.0 C to check quality of the reaction. Amounts of GLA message relative to untransfected control LA-N-2 cells were determined using the BioRad Manager Analysis Software 3.1 and the results were normalized to levels of B2M.

2.7 Western Blot Analysis

Cultures were harvested in log-phase growth and cell pellets were extracted as described above for the AGA enzyme assay. The protein content of extracts was determined by using a BCA Assay Kit (Pierce). Extracts (10 μg per lane) and molecular weight markers (SeeBlue Plus2, InVitrogen) were separated by SDS/PAGE using 4–12% Bis-Tris polyacrylamide gels, transferred to nitrocellulose membranes, and probed with rabbit anti-AGA antibody (a gift from Transkaryotic Therapies, Inc., Cambridge, MA) at a dilution of 1:5000 in TRIS-buffered saline containing 0.1% Tween-20. Protein bands were labeled using HRP-conjugated goat anti-rabbit IgG antibody (Millipore, Temecula, CA) and they were visualized using ECL substrate (Biotool.com, Houston, TX). Chemiluminescence was detected using an Amersham™ 600 digital imager (GE Healthcare Life Sciences, Pittsburgh, PA). Recombinant human AGA (TKT Therapies, Inc.) was used as a positive control at 20 ng per lane.

As a loading control, blots were washed and reprobed with goat anti-actin (1–19) antibody (Santa Cruz Biotechnology, Inc.) at 1:5000, which was detected with HRP-labeled donkey anti-goat IgG (Jackson ImmunoResearch, West Grove, PA), followed by development with ECL substrate and digital imaging.

2.8 Growth Curves

LA-N-2 cultures were trypsinized and seeded at 6,000/cm^2 in duplicate wells of 24-well plates in growth medium. At the designated intervals cells were trypsinized and resuspended in PBS containing nile red (5 μg/ml). Total cell numbers were determined using a Guava PCA flow cytometer equipped with ViaCount® software.

2.9 ACh Release Assay

ACh release was determined by a modification of the method of Bernardini et al.[20]. Cells were seeded in triplicate in 24-well plates at 32,000 cells/cm^2 in growth medium. The next day, medium was changed to serum-free Neurobasal® A (Gibco) supplemented with GlutaMAX™ (0.5 mM), N2 supplement (1%, Life Technologies), leukemia inhibitory factor (5 ug/ml) and choline chloride (100 mM) in order to differentiate the cells and upregulate

ACh production. After 4 days, medium was removed, the cells were washed twice with pre-warmed HEPES-buffered saline and then incubated for 20 min at 37° C with 1.0 ml/well pre-warmed PBS with Ca^{2+} and Mg^{2+}. After the incubation period, an aliquot of the medium was collected, centrifuged at 5,000 × g for 5 min, and the supernatant was stored at −20° C. To stimulate ACh release, incubation medium was replaced with 1.0 ml prewarmed PBS with Ca^{2+} and Mg^{2+} supplemented with 50 mM potassium chloride. After 30 min, the supernatant was collected, centrifuged, and stored at −20° C. The cells in each well were removed by vigorous pipetting with PBS without Ca^{2+} and Mg^{2+}, combined with the cell pellets from the two previous collections, and pelleted at 5000 × g for 5 min. The supernant was removed and the pellets were stored at −20° C.

ACh levels in the collected medium were determined using an Amplex® Red Acetylcholine/Acetylcholinesterase Assay Kit (Molecular Probes, Eugene, OR) according to the manufacturer's instructions. Results from the samples were compared to a standard curve to determine total ACh released. Cell numbers were determined by extracting the DNA from the cell pellet with saline sodium citrate buffer [21] and quantitating total DNA using a Quant-It™ DNA Assay kit (ThermoFisher). ACh release was standardized to total ACh released per hour per μg DNA.

3. Results

3.1 LA-N-2 cells can be differentiated to a neuronal phenotype

LA-N-2 cells are derived from a primary neuroblastoma in a 3 year old female [22]. By incubating with retinoic acid and growth factors, they can be induced to differentiate to neuronal-type cells with characteristics of cholinergic neurons (Fig. 1). The differentiated cells highly express PGP 9.5, a protein marker for neurons [23].

3.2 shRNA-mediated silencing of AGA efficiently reduces AGA mRNA and protein expression in LA-N-2 cells

In order to create a model of Fabry disease we transfected LA-N-2 cells with an shRNA plasmid targeting the second exon of the GLA gene and selected stable transformants with puromycin as described in Methods. Initially, colonies were screened on the basis of AGA activity. The colony with the lowest activity, LA-N-2 Cl 7, was further subcloned to obtain pure populations of transfected cells. Two of the subclones with the lowest AGA activity, LA-N-2 Cl 7-D1 and LA-N-2 Cl 7-C3 were selected for further analysis. In addition, to control for possible off-target effects, we also established a stably–transformed control LA-N-2 cell line that had been transfected with a plasmid that codes for scrambled RNA that does not correspond to any known message. We designated these cells LA-N-2 Negative.

Real-time PCR analysis of the mRNA from exon 2 of AGA showed the amount of normalized AGA message was reduced by 80% in the two subclones and by 70% in the original Clone 7 (Fig. 2). In the negative control, amount of AGA message was not affected compared to the untransfected parent line.

Since protein abundance does not always correlate with reduced protein expression [24], we performed a Western blot of AGA protein levels as described in Methods. The results of a

typical blot are shown in Fig. 2B. Reduction in mRNA levels produced a large reduction in the expression of AGA protein in the gene-silenced cells.

3.3 shRNA-mediated silencing of AGA creates a Fabry phenotype in LA-N-2 cells

Results of a standard enzyme assay for AGA activity are shown in Fig. 3A. The activity of AGA was reduced to 30% of untransfected control in LA-N-2 Clone 7 and to 16% and 12% of untransfected control in subclones 7-C3 and 7-D1, respectively. By contrast, activities of a second lysosomal enzyme, hexosaminidase (HEX), were within control values or higher, indicating the reduction in AGA activity was specific. These levels of reduction in AGA activity were sufficient to cause storage of Gb3 in the cells as demonstrated by immunostaining and FACS analysis (Fig. 3).

Fig. 3B shows a typical result of immunostaining in LA-N-2 CL 7-D1 cells. The cells stain brightly for Gb3. Staining was more diffuse than that typically seen in fibroblasts and appeared to be confined to the cell body. Using the same staining technique, the intensity of staining was compared in LA-N-2 negative, untransfected, and LA-N-2 CL 7 and CL 7-D1 cells by FACS analysis. The results are shown in Fig. 3C. The gene-silenced LA-N-2 clones show a measurable increase in total Gb3 staining, indicating the reduction in enzyme activity was sufficient to produce an accumulation of substrate in these cells.

3.4 siRNA-silenced LA-N-2 cells are functionally impaired

Consistent with findings by other groups for AGA gene-silenced endothelial hybrid cells [25] and cultured renal tubule epithelial cells [26], growth of gene-silenced LA-N-2 cells was significantly slower than control cells (Fig. 4).

Between days 4 and 11, doubling times were 34.2 hrs and 38.3 hrs for untransfected cells and negative controls, respectively, and 50.6 hrs and 45.3 hrs for Clone 7-C3 and CL 7-D1, respectively, indicating a general deficiency in cellular function in the gene-silenced cells.

Since LA-N-2 cells have been well established as a model system for cholinergic neurons [14,27–31], we tested both basal release and potassium-stimulated release of ACh in the silenced cells (Fig. 5). Spontaneous release of ACh into the culture medium was decreased by 67% and 54% in LA-N-2 CL 7 and CL7-D1, respectively, although only the decrease shown by LA-N-2 CL 7 achieved statistical significance ($P < 0.05$). When the cellular membranes were depolarized with an elevated KCl concentration (stimulated release) using 50mM KCl, both gene-silenced clones showed significantly reduced release of ACh compared to untransfected control cultures ($P < 0.05$) (Fig. 5), indicating that neurotransmitter release, a specific neuronal function, is significantly altered in these cells.

4. Discussion

In Fabry disease, neuropathic pain and parasympathetic and sympathetic nervous dysfunction are hallmarks of the disease and greatly affect the quality of life in these patients. However, the cause of this dysfunction is not known. Using gene-silencing techniques, we have established and characterized a neuronal-type cell line that has the

features of Fabry disease including reduced AGA activity and accumulation of the stored substrate, Gb3.

Mutations in the GLA gene may occur anywhere within the AGA protein and have variable effects on enzyme activity, resulting in residual activities that range from undetectable to >20% of control values depending on the assay system used. In one study of kidney function in symptomatic Fabry patients, AGA activity in leukocytes was undetectable in 31 of 49 patients and was 1%–12% of control values in 18 of 49 patients [32], demonstrating that even patients with residual AGA activity can have classical symptoms of Fabry disease. Lukas and co-workers [33] used a plasmid over-expression system to evaluate enzyme kinetics in 171 selected AGA mutations created by site-directed mutagenesis. They showed that mutations that result in AGA enzyme with residual activity up to 20% of wild-type were associated with the presence of classical Fabry symptoms in 85% of the patients with these mutations. In our model, reduction of AGA activity to 12%–15% of wild-type (Fig 3A) was similar to the amount of residual activity of genetically-mutant enzyme found in some patients expressing symptoms of Fabry disease. Therefore, we expect that the functional impairment of AGA activity in this model will be sufficient to provide an understanding of functional defects found in symptomatic patients.

The reduced growth rate we found in our gene-silenced LA-N-2 cells (Fig. 4) is consistent with findings by other groups. Shu et al found in the hybrid endothelial cell line, EA.hy926, transient silencing of AGA expression with dicer siRNA induced storage of Gb3 and caused a significant reduction in the proliferation of the gene-silenced cells over 8 days. By contrast, transfection with dicer siRNA against a related enzyme, b-glucocerebrosidase, or an unrelated enzyme, glyceraldehyde 3-phosphate dehydrogenase, had no effect on growth [25]. In both primary and immortalized human tubular epithelial cells stably transfected with shRNA against AGA, Thomaidis et al found a 50% reduction in growth rate compared to control [26].

Recently Lakoma and co-workers reported a detailed study of proliferation markers in fibroblasts derived from Fabry patients and normal controls [34]. They demonstrated that growth of AGA mutant fibroblasts was affected by the presence of lipid in the form of serum in the culture medium. They found expression of Ki-67, a marker for cell proliferation, was significantly lower in Fabry fibroblasts compared to control when both were cultured in standard serum levels of 10%, but this difference normalized when serum levels were lowered to 1%. By contrast, a second marker of proliferation, $Ph3^{+}$, remained unchanged and was not significantly different from control. The influence of Gb3 accumulation on cell cycle regulation remains to be determined and is most likely affected by both cell type and the environmental milieu. Differences in proliferative rate in our gene silenced cells compared to both untransfected controls and negative plasmid transfected controls offers an additional model for examining this question.

Of particular interest is our finding that in cells with knocked-down AGA activity, release of the neurotransmitter ACh is significantly reduced (Fig. 5). ACh is synthesized in neurons from choline and acetyl-CoA. Acetyl-CoA is produced in mitochondria as a product of the citric acid cycle and transported across the mitochondrial membrane into the cytoplasm

where it is complexed with choline to form ACh by the action of choline acetyl transferase (ChAT) [35]. ACh is packaged in small synaptic vesicles by the activity of vesicular acetylcholine transporter (VAChT) [36]. Upon stimulation of the nerve, influx of calcium causes fusion of the vesicles with the plasma membrane and release of the stored neurotransmitter into the synaptic space.

The mechanism of the reduction in ACh release in the gene-silenced LA-N-2 is probably complex. In Fabry disease, Lucke *et al.* have demonstrated that mitochondrial energy production is reduced in fibroblasts from Fabry patients [37]. Such impairment may result in reduced synthesis of acetyl-CoA, limiting the amount of ACh formed in the LA-N-2 cells. Increase in expression of Gb3 in the plasma membrane of AGA gene-silenced endothelial cells has been documented [26]. Increased amounts of Gb3 in glycolipid membranes affect the mechanical properties of the membrane by increasing bending stiffness [38]. Changes in the mechanical properties of cellular membranes could potentially influence vesicle formation and fusion. Park and co-workers have shown intermediate-conductance Ca^{2+}-activated K^+ (KCa3.1) channels are both down-regulated and functionally inhibited in endothelial cells from a mouse model of Fabry disease [39]. Reduction in Ca^{2+} influx may also affect release of ACh.

Recent advances in immunostaining for acetylcholine-related proteins such as VAChT have shown that localization of cholinergic neurons in the peripheral nervous system is more extensive than was previously thought [40]. Using immunostaining for peripheral acetylcholine transferase (pChAT) in rat skin, Hanada et al. [41] demonstrated that cholinergic neurons are associated with eccrine sweat glands, blood vessels, hair follicles, and cutaneous sensory nerve endings [41], all of which are affected in Fabry disease. In addition, the same authors found extensive pChAT staining in DRG neuronal cells. Since DRG neurons are associated with the perception of pain [42] and accumulation of Gb3 in DRG of Fabry patients has been demonstrated [8], these results, as well as our finding of impaired ACh release in the LA-N-2 cells, suggests that the involvement of ACh in neuropathic pain in Fabry patients warrants further investigation.

In Fabry patients, hypohidrosis is a hallmark of the disease. Sweat glands are surrounded by sympathetic nerve terminals that are mainly cholinergic [43] which stimulate the release of sweat in response to environmental changes. Using immunostaining with the broadly-expressed neuronal marker, PGP 9.5, Schiffmann and Scott demonstrated that the innervation density of sweat glands in skin biopsies from Fabry patients is not reduced compared to normal controls [44] and therefore the hypohidrosis found in Fabry disease cannot be explained by a decrease in the number of nerve endings. However, since ACh is the main neurotransmitter used in the stimulation of sweat release [43], functional impairment in the release of ACh by the nerve endings, such as that found in our model system (Fig. 5), may help explain this aspect of the disease.

Development of a neuronal model in Fabry disease is important to understanding the pathophysiology of this disease in mechanistic detail. We hope that the model system we have described will help to decipher the neuronal dysfunction associated with Fabry disease. Using this model system, we can now investigate potential sources of neuronal dysfunction

in Fabry disease and test effects of various treatments. Further experiments are in progress to determine the cause of reduced ACh release in the gene-silenced LA-N-2 cells.

Acknowledgments

This research was supported in part by the NIDDK Intramural Research Program and the NINDS Intramural Research Program at the National Institutes of Health, Bethesda, MD, and by Pfizer Inc., New York, NY (grant number IIR #WI171341 to UHS).

Abbreviations

4-MU	4-methylumbelliferone
AGA	alpha-galactosidase A
ACh	acetylcholine
B2M	beta-2-microglobulin
CTNF	ciliary neurotrophic factor
FACS	fluorescence activated cells sorting
HEX	hexosaminidase
HRP	horseradish peroxidase
Gb3	globotriaosylceramide
GCS	GemCell™ Calf Serum
lyso-Gb3	globotriaosylsphingosine
pChAT	peripheral acetylcholine transferase
qRT-PCR	quantitative real-time reverse-transcription polymerase chain reaction
RFU	relative fluorescence units
shRNA	short-hairpin RNA
VAChT	vesicular acetylcholine transporter

References

1. Tuttolomondo A, Pecoraro R, Simonetta I, Miceli S, Pinto A, Licata G. Anderson-Fabry disease: a multiorgan disease. Curr Pharm Des. 2013; 19:5974–5996. [PubMed: 23448451]
2. Saito S, Ohno K, Sakuraba H. Fabry-database.org: database of the clinical phenotypes, genotypes and mutant α-galactosidase A structures in Fabry disease. J Hum Genet. 2011; 56:467–468. [PubMed: 21412250]
3. Schiffmann, R.; Moore, D. [accessed March 9, 2016] Neurological manifestations of Fabry disease - Fabry Disease - NCBI Bookshelf. n.d. http://www.ncbi.nlm.nih.gov/books/NBK11602/
4. Cable WJL, Kolodny EH, Adams RD. Fabry disease impaired autonomic function. Neurology. 1982; 32:498–498. [PubMed: 6803189]

5. Tabira T, Goto I, Kuroiwa Y, Kikuchi M. Neuropathological and biochemical studies in Fabry's disease. Acta Neuropathol (Berl). 1974; 30:345–354. [PubMed: 4217553]
6. Scott LJC, Griffin JW, Luciano C, Barton NW, Banerjee T, Crawford T, McArthur JC, Tournay A, Schiffmann R. Quantitative analysis of epidermal innervation in Fabry disease. Neurology. 1999; 52:1249–1249. DOI: 10.1212/WNL.52.6.1249 [PubMed: 10214752]
7. Schiffmann R. Neuropathy and Fabry disease: pathogenesis and enzyme replacement therapy. Acta Neurol Belg. 2006; 106:61. [PubMed: 16898255]
8. Gadoth N, Sandbank U. Involvement of dorsal root ganglia in Fabry's disease. J Med Genet. 1983; 20:309–312. [PubMed: 6413695]
9. Aerts JM, Groener JE, Kuiper S, Donker-Koopman WE, Strijland A, Ottenhoff R, van Roomen C, Mirzaian M, Wijburg FA, Linthorst GE, et al. Elevated globotriaosylsphingosine is a hallmark of Fabry disease. Proc Natl Acad Sci. 2008; 105:2812–2817. [PubMed: 18287059]
10. Choi L, Vernon J, Kopach O, Minett MS, Mills K, Clayton PT, Meert T, Wood JN. The Fabry disease-associated lipid Lyso-Gb3 enhances voltage-gated calcium currents in sensory neurons and causes pain. Neurosci Lett. 2015; 594:163–168. DOI: 10.1016/j.neulet.2015.01.084 [PubMed: 25697597]
11. Schueler U, Kolter T, Kaneski CR, Blusztajn JK, Herkenham M, Sandhoff K, Brady RO. Toxicity of glucosylsphingosine (glucopsychosine) to cultured neuronal cells: a model system for assessing neuronal damage in Gaucher disease type 2 and 3. Neurobiol Dis. 2003; 14:595–601. DOI: 10.1016/j.nbd.2003.08.016 [PubMed: 14678774]
12. Tuttolomondo A, Pecoraro R, Simonetta I, Miceli S, Arnao V, Licata G, Pinto A. Neurological complications of Anderson-Fabry disease. Curr Pharm Des. 2013; 19:6014–6030. [PubMed: 23448452]
13. Lakomá J, Rimondini R, Donadio V, Liguori R, Caprini M. Pain Related Channels Are Differentially Expressed in Neuronal and Non-Neuronal Cells of Glabrous Skin of Fabry Knockout Male Mice. PLoS ONE. 2014; 9:e108641.doi: 10.1371/journal.pone.0108641 [PubMed: 25337704]
14. Richardson I, Liscovitch Mordechai, Blusztajn Jan Krzysztof. Acetylcholine synthesis and secretion by LA-N-2 human neuroblastoma cells. Brain Res. 1989; 476:323–331. [PubMed: 2702472]
15. [accessed March 21, 2016] GPP Web Portal - Clone Details. n.d. http://www.broadinstitute.org/rnai/public/clone/details?cloneId=TRCN0000303790
16. Zinman LH, Lawrance G, Wang W, Verge VMK, Dow KE, Maurice DH, Richardson PM, Riopelle RJ. Collaborative and reciprocal effects of ciliary neurotrophic factor and nerve growth factor on the neuronal phenotype of human neuroblastoma cells. J Neurochem. 1998; 70:1411–1420. [PubMed: 9523557]
17. Kaneski CR, Schiffmann R, Brady RO, Murray GJ. Use of lissamine rhodamine ceramide trihexoside as a functional assay for alpha-galactosidase A in intact cells. J Lipid Res. 2010; 51:2808–2817. DOI: 10.1194/jlr.D007294 [PubMed: 20526001]
18. Mayes JS, Scheerer Julia B, Sifers Richard N, Donaldson Mark L. Differential assay for lysosomal alpha-galactosidases in human tissues and its application to Fabry's disease. Clin Chem Acta. 1981; 112:247–251.
19. Schueler U, Kaneski C, Remaley A, Demosky S, Dwyer N, Blanchette-Mackie J, Hanover J, Brady R. A Short Synthetic Peptide Mimetic of Apolipoprotein A1 Mediates Cholesterol and Globotriaosylceramide Efflux from Fabry Fibroblasts. JIMD Rep. 2015; doi: 10.1007/8904_2015_507
20. Bernardini N, Tomassy GS, Tata AM, Augusti-Tocco G, Biagioni S. Detection of basal and potassium-evoked acetylcholine release from embryonic DRG explants. J Neurochem. 2004; 88:1533–1539. DOI: 10.1046/j.1471-4159.2003.02292.x [PubMed: 15009654]
21. Otto WR. Fluorimetric DNA assay of cell number. Epidermal Cells Methods Protoc. 2005:251–262.
22. Seeger RC, Rayner SA, Banerjee A, Chung H, Laug WE, Neustein HB, Benedict WF. Morphology, growth, chromosomal pattern, and fibrinolytic activity of two new human neuroblastoma cell lines. Cancer Res. 1977; 37:1364–1371. [PubMed: 856461]

23. Thompson RJ, Doran JF, Jackson P, Dhillon AP, rode J. PGP 9.5 -- a new marker for vertebrate neurons and neuroendocrine cells. Brain Res. 1983; 278:224–228. [PubMed: 6640310]
24. Greenbaum D, Colangelo C, Williams K, Gerstein M. Comparing protein abundance and mRNA expression levels on a genomic scale. Genome Biol. 2003; 4:117. [PubMed: 12952525]
25. Shu L, Vivekanandan-Giri A, Pennathur S, Smid BE, Aerts JMF, Hollak CE, Shayman JA. Establishing 3-nitrotyrosine as a biomarker for the vasculopathy of Fabry disease. Kidney Int. 2014; 86:58–66. [PubMed: 24402087]
26. Thomaidis T, Relle M, Golbas M, Brochhausen C, Galle PR, Beck M, Schwarting A. Downregulation of α-galactosidase A upregulates CD77: functional impact for Fabry nephropathy. Kidney Int. 2009; 75:399–407. [PubMed: 19037253]
27. Yeh HH, Notter MFD, Kordowerr JH, Gash DM. Snyapse-competence of LA-N-2 human neuroblastoma cells in cocultue with rat striated muscle cells. Neuoscience. 1988; 27:309–315.
28. Singh IN, Sorrentino G, McCartney DG, Massarelli R, Kanfer JN. Enzymatic activites during differentiation of the human neuroblastoma cells, LA-N-1 and LA-N-2. J Neurosci Res. 1990; 25:476–485. [PubMed: 2352289]
29. Rylett RJ, Goddard S, Lambros A. Regulation of Expression of Cholinergic Neuronal Phenotypic Markers in Neuroblastoma LA-N-2. J Neurochem. 1993; 61:1388–1397. [PubMed: 8376993]
30. Crosland RD. Differentiation agents enhance cholinergic characteristics of LA-N-2 human neuroblastoma cells. Life Sci. 1996; 58:1987–1994. [PubMed: 8637428]
31. North WG, Fay MJ, Du J, Cleary M, Gallagher JD, McCann FV. Presence of functional NMDA receptors in a human neuroblastoma cell line. Mol Chem Neuropathol Spons Int Soc Neurochem World Fed Neurol Res Groups. Neurochem Cerebrospinal Fluid. 1997; 30:77–94.
32. Branton MH, Schiffmann R, Sabnis SG, Murray GJ, Quirk JM, Altarescu G, Goldfarb L, Brady RO, Balow JE, Austin HA III, et al. Natural history of Fabry renal disease: influence of α-galactosidase A activity and genetic mutations on clinical course. Medicine (Baltimore). 2002; 81:122–138. [PubMed: 11889412]
33. Lukas J, Giese AK, Markoff A, Grittner U, Kolodny E, Mascher H, Lackner KJ, Meyer W, Wree P, Saviouk V, Rolfs A. Functional Characterisation of Alpha-Galactosidase A Mutations as a Basis for a New Classification System in Fabry Disease. PLoS Genet. 2013; 9:e1003632.doi: 10.1371/journal.pgen.1003632 [PubMed: 23935525]
34. Lakomá J, Donadio V, Liguori R, Caprini M. Characterization of Human Dermal Fibroblasts in Fabry Disease: VRACs EXPRESSION IN FABRY DISEASE. J Cell Physiol. 2016; 231:192–203. DOI: 10.1002/jcp.25072 [PubMed: 26058984]
35. Dobransky T, Rylett RJ. A model for dynamic regulation of choline acetyltransferase by phosphorylation. J Neurochem. 2005; 95:305–313. DOI: 10.1111/j.1471-4159.2005.03367.x [PubMed: 16135099]
36. Prado VF, Roy A, Kolisnyk B, Gros R, Prado MAM. Regulation of cholinergic activity by the vesicular acetylcholine transporter. Biochem J. 2013; 450:265–274. DOI: 10.1042/BJ20121662 [PubMed: 23410039]
37. Lücke T. Fabry disease: reduced activities of respiratory chain enzymes with decreased levels of energy-rich phosphates in fibroblasts. Mol Genet Metab. 2004; 82:93–97. DOI: 10.1016/j.ymgme.2004.01.011 [PubMed: 15110329]
38. Yamamoto A, Abuillan W, Burk AS, Körner A, Ries A, Werz DB, Demé B, Tanaka M. Influence of length and conformation of saccharide head groups on the mechanics of glycolipid membranes: Unraveled by off-specular neutron scattering. J Chem Phys. 2015; 142:154907.doi: 10.1063/1.4918585 [PubMed: 25903910]
39. Park S, Kim JA, Joo KY, Choi S, Choi EN, Shin JA, Han KH, Jung SC, Suh SH. Globotriaosylceramide leads to KCa3.1 channel dysfunction: a new insight into endothelial dysfunction in Fabry disease. Cardiovasc Res. 2011; 89:290–299. DOI: 10.1093/cvr/cvq333 [PubMed: 20971723]
40. Schäfer MK-H, Eiden LE, Weihe E. Cholinergic neurons and terminal fields revealed by immunohistochemistry for the vesicular acetylcholine transporter. II. The peripheral nervous system. Neuroscience. 1998; 84:361–376. DOI: 10.1016/S0306-4522(97)80196-0 [PubMed: 9539210]

41. Hanada K, Kishimoto S, Bellier JP, Kimura H. Peripheral choline acetyltransferase in rat skin demonstrated by immunohistochemistry. Cell Tissue Res. 2012; 351:497–510. DOI: 10.1007/s00441-012-1536-z [PubMed: 23250574]

42. Guha D, Shamji MF. The Dorsal Root Ganglion in the Pathogenesis of Chronic Neuropathic Pain. Neurosurgery. 2016; 63:118–126. DOI: 10.1227/NEU.0000000000001255 [PubMed: 27399376]

43. Shibasaki M, Crandall CG. Mechanisms and controllers of eccrine sweating in humans. Front Biosci Sch Ed. 2010; 2:685–696.

44. Schiffmann R, Scott LJC. Pathophysiology and assessment of neuropathic pain in Fabry disease. Acta Pædiatrica. 2002; 91:48–52. DOI: 10.1111/j.1651-2227.2002.tb03110.x

Highlights

- Fabry disease is caused by a deficiency of lysosomal alpha-galactosidase A (AGA).
- Stable transfection of shRNA silenced AGA expression in the neuronal cell line LA-N-2.
- Gene-silenced LA-N-2 cells have reduced AGA activity and accumulate Gb3.
- Gene-silenced LA-N-2 show impaired neurotransmitter release and poor growth.

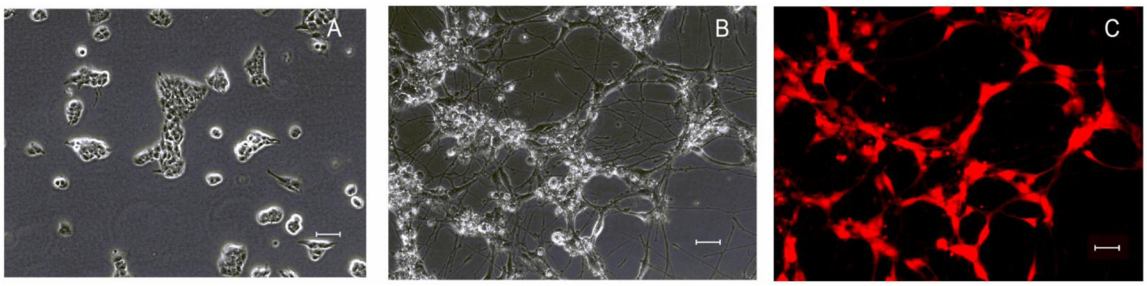

Fig 1.

LA-N-2 cells can be differentiated to a neuronal cell type. (A) LA-N-2 cells before differentiation. (B) LA-N-2 after 4 days incubation with differentiation medium as described in Methods. (C) Differentiated cells stained for PGP 9.5, a pan-neuronal marker. Scale bar = 50 um.

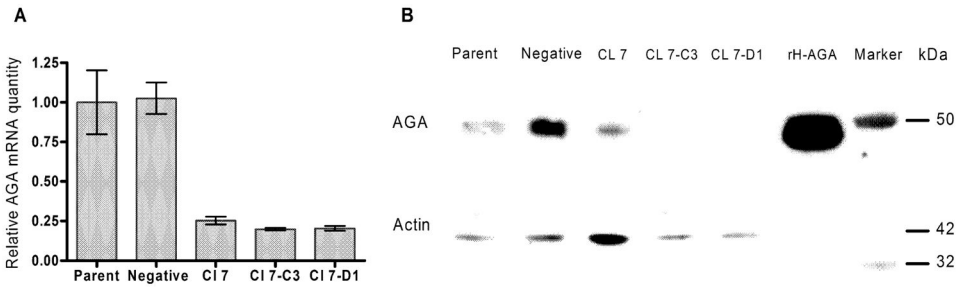

Fig 2.

Gene silencing in LA-N-2 cells. (A) RT-PCR for AGA message was performed as described in Methods. Values represent means of duplicate samples. Results were normalized to B2M mRNA levels and results are expressed as the normalized amount of mRNA relative to non-transfected controls. (B) Western blot of AGA protein expression. Amount of immunoreactive AGA was reduced in the gene-silenced cells. Actin levels were used as a loading control.

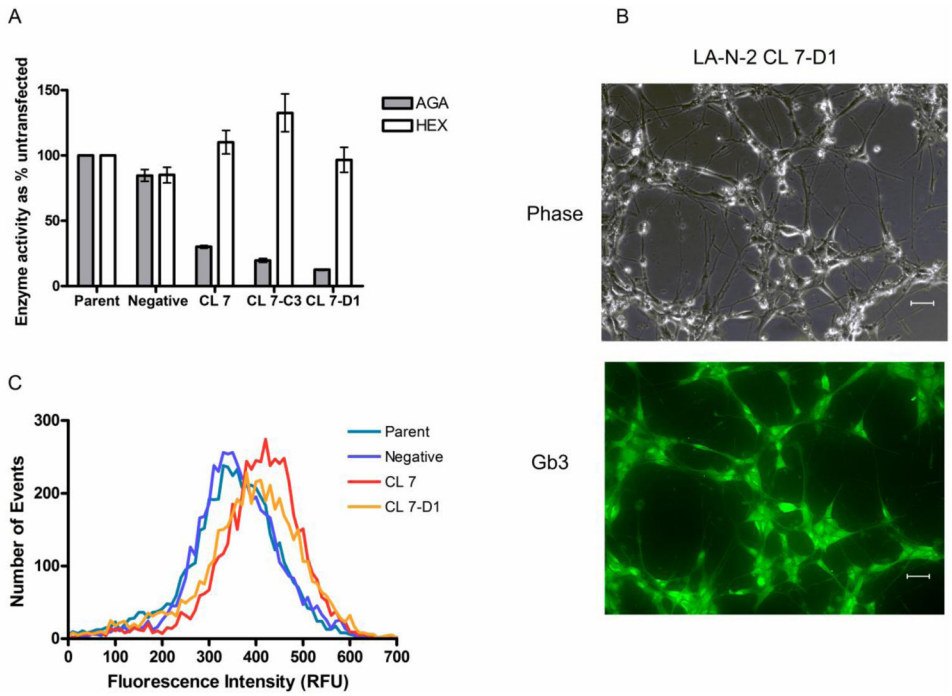

Fig. 3.

Deficiency of AGA activity in gene-silenced LA-N-2 cells. (A) AGA enzyme activity in cellular homogenates. Results are expressed as % activity relative to untransfected control. Bars are averages of triplicate cultures +/− SD. (B) Immunostaining for Gb3 in LA-N-2 CL-7D1 cells shows bright labeling within the cell body. Scale bar = 50 um. (C) FACS analysis of gene-silenced LA-N-2 cells immunostained for Gb3 shows increased staining intensity for Gb3 in gene-silenced clones compared to controls.

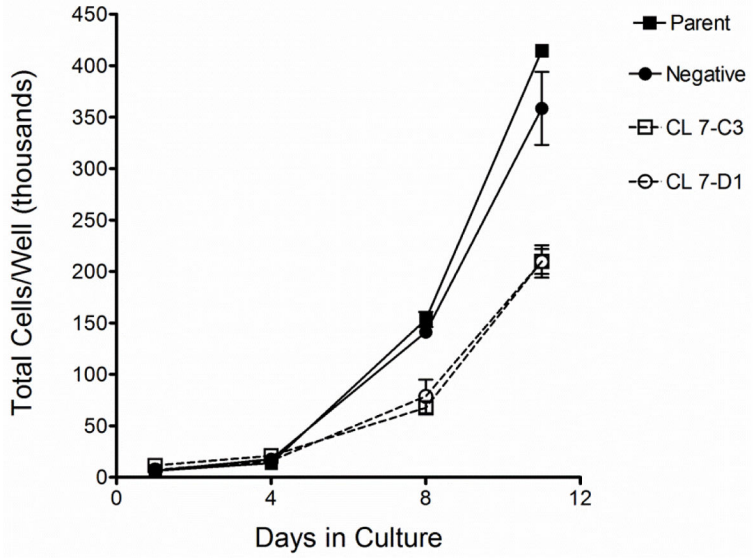

Fig. 4.

Growth curve for gene-silenced LA-N-2 cells and controls. Cells were seeded at equal numbers and counted every 3–4 days as described in Methods. Points are averages of triplicate wells +/− SD.

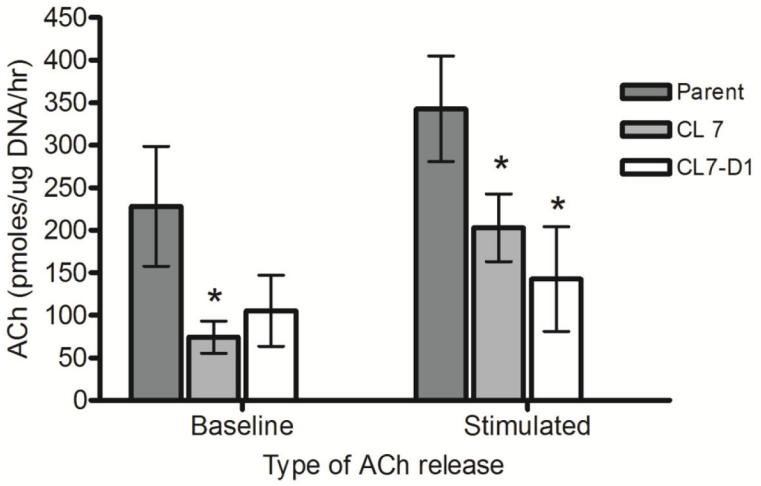

Fig. 5.

Baseline and KCl-stimulated release of ACh in gene-silenced LA-N-2 clones. Release of ACh into the medium of differentiated LA-N-2 cultures was determined as described in Methods at baseline and again after KCl stimulation. Amount of ACh was normalized to cell number measured by DNA quantitation. Results are means of triplicate wells +/− standard deviation. *($P < 0.05$) compared to parent.